IL NUOVO CIMENTO **43 C** (2020) 142
DOI 10.1393/ncc/i2020-20142-0

COLLOQUIA: SIRR 2020

Thermoluminescent dosimeters (TLDs-100) calibration for dose verification in photon and proton radiation therapy

V. D'AVINO(1)(*), M. CARUSO(2), C. ARRICHIELLO(3), G. AMETRANO(3), G. LA VERDE(1)(4)(5), P. MUTO(3), E. SCIFONI(6), F. TOMMASINO(6)(7) and M. PUGLIESE(1)(4)

(1) *National Institute of Nuclear Physics, Section of Naples - Naples, Italy*
(2) *Department of Electrical Engineering and Information Technologies, University of Naples Federico II - Naples, Italy*
(3) *Radiotherapy Unit, Istituto Nazionale Tumori, IRCCS, Fondazione G. Pascale - Naples, Italy*
(4) *Department of Physics "E. Pancini", University of Naples Federico II - Naples, Italy*
(5) *Department of Pharmacy, University of Naples Federico II - Naples, Italy*
(6) *TIFPA-INFN, Trento Institute for Fundamental Physics and Applications, Istituto Nazionale di Fisica Nucleare - Trento, Italy*
(7) *Department of Physics, University of Trento - via Sommarive, 14, Trento, Italy*

received 25 January 2021

Summary. — Thermoluminescent dosimeters (TLDs) are practical, accurate, and precise tools for point dosimetry in medical physics applications. TLDs are nowadays extensively used to measure dose in conformal radiation therapy in order to guarantee the safety of the treatment. Several national and international organizations recommend checking the effective dose delivered to an individual patient by means of *in vivo* dosimetry. Modern radiotherapy techniques employing both photon and ion beams exhibit excellent target conformation throught high steep-dose gradients between tumour and adjacent organs and tissues. In this context, catching potential dose errors and uncertainties in treatment delivering is the first step to ensure the optimization of the treatment plan. This study shows the results of the characterization of TLDs-100 at two Italian facilities devoted to advanced radiation treatments with photon and proton therapy. The individual sensitivity factor was determined, and the calibration curves were carried out in the dose range 0–20 Gy. By the analysis of the dose response curves, the linear region was identified under the dose level of 10 Gy. Characterization of the TLDs-100 has enabled their use for *in vivo* dosimetry especially in the dose range corresponding to the linear region of the dose response curves.

(*) Corresponding author. E-mail: vittoria.davino@na.infn.it

1. – Introduction

Thermoluminescent dosimeters (TLDs) are widely used in clinical application to measure the radiation dose because of their physical and dosimetric characteristics (*i.e.*, availability, ease of handling, reusability, precision, tissue equivalence) [1-4]. Their small size allows obtaining point dose measurements with high resolution on phantom and patient as well. In particular TLD-100 dosimeters, based on lithium fluoride doped with magnesium and titanium (LiF:Mg, Ti), exhibiting low signal fading (5–10% per year) and high sensitivity to different radiation qualities, are suitable for dose verification in radiation therapy (RT) beams [5-8]. Furthermore, the wide linear response range (10 μGy–10 Gy), is the reason why TLDs-100 are frequently chosen to evaluate the dose distribution in routine computed tomography scans [9-11].

In the last years, development of advanced radiation therapy techniques, such as intensity-modulated radiation therapy (IMRT), stereotactic radiotherapy (SRT), intraoperative electron radiation therapy (IOERT), proton therapy, has been rapidly spreading worldwide. The modern treatment photon-beam–based modalities achieve a more precise conformation of the radiation dose to the target volume than the conventional 3D-RT: they deliver the treatment plan through numerous radiation fields arranged in complex geometry, eventually combined with a variation of intensity from different directions [12-14]. On the other hand, using proton beams an excellent dose conformation is achieved, thanks to the properties of charged particles interaction with matter, which causes a very rapid energy loss in the last few millimetres of penetration. The so-called Bragg peak consists in a pronounced maximum of dose deposition in a localized region, resulting in a reduced integral dose to normal tissue [15-17].

Charged particles produce different biological effects compared to photons [18, 19] depending on the linear energy transfer (LET) and track structure models in the living cells, as demonstrated by *in vitro* and *in vivo* experiments [20, 21].

The potential of advanced radiotherapy modalities lies in the improvement of target dose coverage combined with the sparing of normal healthy tissue by implementing a dose escalation at the interface between the target and the surrounding structures. A twofold clinical benefit ensues: increase of the local tumour control and reduction of acute and long-term toxicity to the healthy organs. In this regard, charged particle therapy is the treatment of choice for those tumours which are located close to critical structures such as spinal cord, eyes, and brain, as well as for paediatric malignancies [15, 17]. Some studies demonstrated the correlation between the absorbed dose and both local tumour control and normal tissue complications probability [22-24].

When a very accurate dose delivery to the tumour is required and critical organs at risk are potentially involved in high dose field, in order to ensure that the patient is treated safely and effectively, dosimetric measurements are necessary. To this end, *in vivo dosimetry* routine is highly recommended by quality assurance (QA) guidelines stated by national and international organizations [25, 26]. Diodes and thermoluminescence dosimeters are the most common detector types employed for *in vivo* dosimetry since they are small, safe and unobtrusive. They can be positioned on the patient's skin, in body cavities or behind the patient. Furthermore, many phantoms readily accommodate these detectors, especially TLDs [27]. Over diodes, TLDs have the main advantage that they do not need to be connected to any electrometer during measurements. For these reasons, TLD dosimetry is the method of choice in routine clinical use in many facilities for over 30 years. A wide literature concerns the use of TLDs in conventional radiation therapy describing details on the physical characteristics and practical aspects of their

clinical use [2-4, 28]. However, due to the relative recent development of charged particle therapy for cancer treatment, the use of TLDs in the field of proton therapy is less popular. For this reason, to the best of our knowledge, the response of TLDs irradiated by clinical proton beams has not been investigated yet.

For accurate *in vivo* dosimetry, dose calibration of the thermoluminescent dosimeters must be ideally performed at the same beam quality used for the subsequent dose measurement. In fact, the TLD response is beam-energy– and modality-dependent [29]. In this work TLD-100 dosimeters were characterized with both 6 and 15 MeV photon beams as well as with a proton beam of a maximum energy of 230 MeV, currently intended for radiotherapy applications. The TLD's investigation was performed in the dose range 0–20 Gy useful to verify the nonlinearity behaviour demonstrated in some literature works for photon beams [30, 31] and to investigate the dose responses curves in the proton beam. The goal of the work was to characterize several batches of TLDs-100 through the investigation of the dose response functions to obtain their calibration curves. Each characterized batch can then be used for dosimetric measurement at the facilities involved in the study.

2. – Materials and methods

2˙1. *Irradiation facilities and dosimeters selection.* – Three sets of TLDs-100 have been characterized in both photon and proton beam at two national facilities. Elekta Synergy Linear Accelerator (Elekta Instrument AB Stockholm) was available at the Radiotherapy Department of the National Cancer Institute-IRCCS "Fondazione G. Pascale" in Naples equipped with a photon beam source of optional nominal energy selection of 6 and 15 MV. A dose rate of 200 MU/min was set for the irradiations.

At the Trento proton therapy centre, a commercial 230 MeV cyclotron produced by IBA (Proteus Plus, IBA, Belgium) is installed. It is equipped with an energy selection system allowing the transport of any energy in the range 70–228 MeV. A detailed description of the proton beam delivery system is reported in ref. [32].

One set (A) of 40 TLDs-100 already used for irradiation experiments at the Laboratory of Radioactivity (LaRa), Department of Physics of the University of Naples Federico II, and two sets of 53 TLDs (B and C) from a total of 106 dosimeters of a virgin batch, were selected for the study. The chips, produced by the Harshaw Company, have the following physical characteristics: dimensions of $3.2 \times 3.2 \times 0.89\,\mathrm{mm}^3$, spatial resolution of 2 mm, density of $2.64\,\mathrm{g/cm}^3$.

Each TLDs of the virgin batch was coded and subjected to three pre-irradiation annealing cycles as recommended by the producer for best results before initial use. Subsequently, the annealing was repeated prior to each irradiation, following the standard procedure: 1 h heating in an oven at 400 °C; cooling at room temperature; 2 h heating in an oven at 100 °C; cooling at room temperature [33].

As first step of TLDs characterization of each set, the sensitivity factor S_i has been determined in order to carry out their individual response. To this end, all dosimeters were accommodated in a water-equivalent housing and irradiated with a planned dose of 2 Gy at 3 cm depth in a plexiglas (PMMA) phantom. 5 cm of backscattering PMMA material were employed. TLDs were exposed to a 6 MeV photon beam with the beam size of $10 \times 10\,\mathrm{cm}^2$ at a distance of 100 cm from the source (source-to-axis distance technique). The sensibility to attribute to each detector was calculated according to the

following definition:

$$S_i = \frac{R_i}{\overline{R}}, \tag{1}$$

where R_i is the TLD readout of the i-th detector and $\overline{R}$ is the mean of all R_i values. Any dosimeter with a relative sensitivity value greater than $\pm 10\%$ of the mean value must be rejected [34].

A thermoluminescent signal of each dosimeter was obtained from a manual TLD reader, Harshaw model 3500, installed at LaRa. The reading was performed at least 24 h after the irradiation. The reading cycle consists of a linear warming up with a ramp of $5\,^{\circ}\mathrm{C} \cdot \mathrm{s}^{-1}$ starting from 100 °C up to 300 °C. The glow curve was acquired over 40 seconds. A continuous nitrogen flow ensures the reduction of chemiluminescence and spurious signals not related to the irradiation [31].

2˙2. *Irradiation experiment.* – For photon irradiation, the TLDs for each set were divided in 7 groups containing at least 5 TLDs and irradiated with single dose values (0.5, 1, 2, 5, 8, 12 Gy). The irradiation was performed with the same experimental set-up and procedure described for TLDs sensitivity determination (fig. 1).

For proton irradiation, the TLDs of each set were divided into 9 groups containing at least 3 TLDs and they were irradiated with single dose values up 20 Gy (1, 2, 5, 8, 10, 12, 15, 20 Gy). In each measurement session, at least one TLD was not exposed to radiation in order to measure the background signal (readings for the 0 cGy dose). The TLDs were accommodated in a cavity on a plexiglas slab of the water-equivalent phantom (RW3 slab phantom), specially designed for the insertion of an ionization chamber. Aiming at reducing the effects of backscattered radiation and at replacing the adequate conditions of electronic equilibrium, 10 cm thickness of solid water slabs (by Gammex Inc., Middleton, WI) were placed on the treatment bed while 2.1 cm of RW3 slab phantom was put above the slab hosting the TLDs (fig. 2, right panel). Each dose point was separately

Fig. 1. – Pictures of photon irradiation set-up. Left panel: slab of PMMA phantom with TLDs housed in the water-equivalent disk. Right panel: wafer-like configuration, packaging the disk between 5 cm below and 3 cm above PMMA slab phantom. The lines crossing the center of the disk are the position lasers.

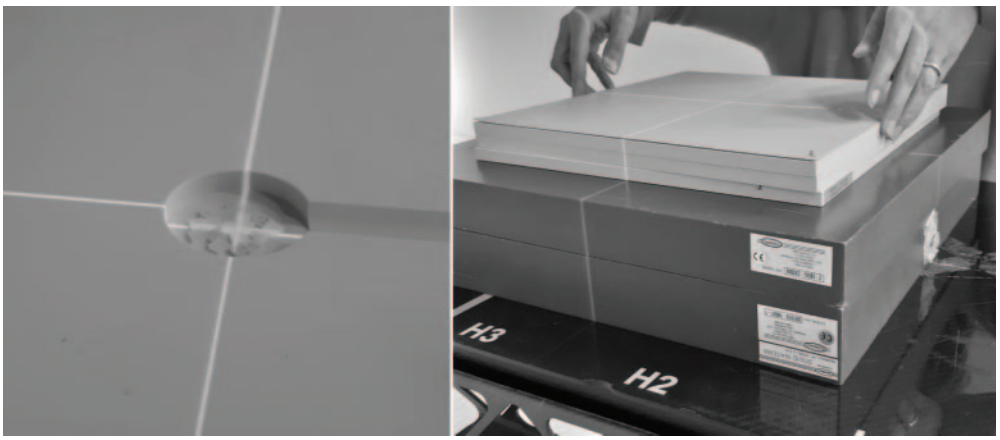

Fig. 2. – Pictures of proton irradiation set-up. Left panel: slab of RW3 phantom with TLDs inserted in the cavity. Right panel: "wafer" configuration with RW3 slab phantom containing TLD between 10 cm of solid water below and 2.1 cm of RW3 slab phantom above. The lines crossing the center of the slab hosting the TLDs are the position lasers.

measured by a Markus parallel plate ionization chamber connected to a PTW-UNIDOS electrometer to verify the accuracy of the delivered dose.

2˙3. *Statistical analysis*. – For each dose energy measurement, the mean response and standard error for each TLD's group were calculated.

For all beams, regression analysis was performed on TLD response as a function of delivered dose. The goodness of the fit was evaluated by the R^2 coefficient. In order to determine the best trend of the calibration curves, fits were performed by both linear and second-order polynomial functions. A linear fit was performed in the dose range 0–8 Gy in order to verify the linearity of TLD dose response useful for clinical application.

3. – Results and discussion

The range of S_i factor for set A, B and C were reported in table I.

Only one TLD of set A was found having $S_i < 0.9$ so it was excluded from dose irradiation. Similarly, from set C two TLDs were excluded because their S_i was greater than $\pm 10\%$ of the mean value.

TABLE I. – *Sensitivity range for each TLD set.*

TLD set	S_i range
A	0.88–1.05
B	0.95–1.09
C	0.65–1.80

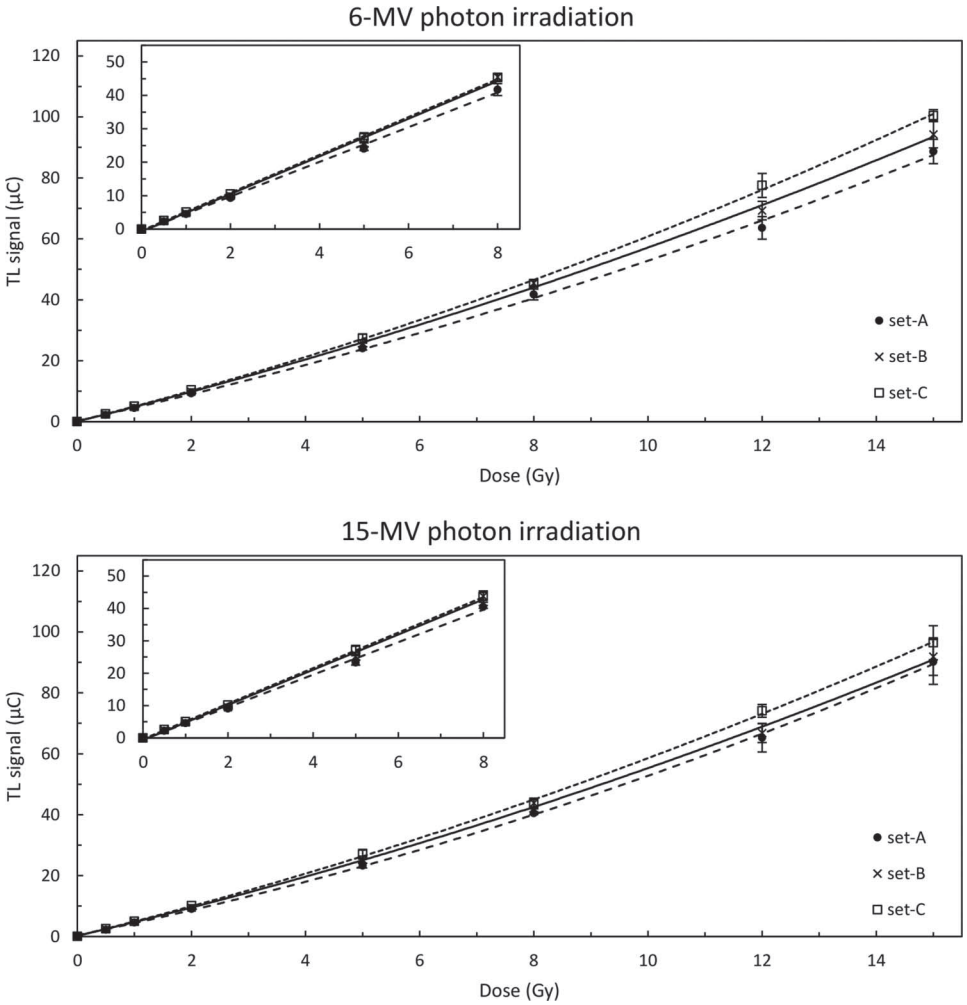

Fig. 3. – Calibration curves of TLDs exposed to 6 and 15 MV photon beams. The main graph reports the quadratic fit for each TLD set in the dose range 0–15 Gy. The inset shows the linear fit of the thermoluminescent response as a function of the radiation dose in the dose range 0–8 Gy.

In fig. 3 the TL signal *versus* dose curves fitted with second-order polynomials for each batch in the photon beam was depicted. The linear fit of the thermoluminescent response as a function of the radiation dose was also plotted in the dose range 0–8 Gy (inset in fig. 3).

The calibration curves for 6 and 15 MV photon beams (see insets in fig. 3) show that the fitting curve has a linear behaviour below 10 Gy, in line with the well-known published results [7, 8, 35, 36].

Concerning the thermoluminescent response in the proton field, we observed similar behaviour as in photon beam (fig. 4).

Table II shows the linear and second-order polynomial functions and the statistical parameters resulting from the best-fit regression analysis performed in the dose range

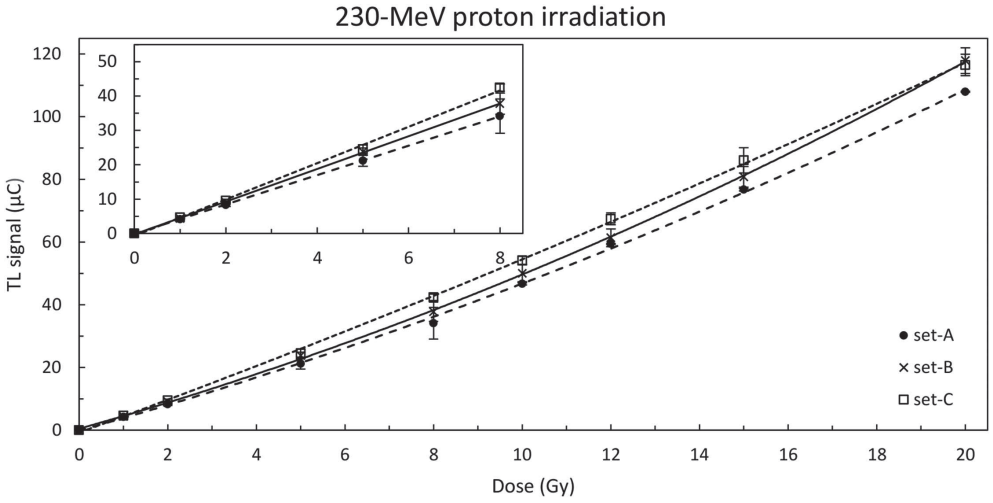

Fig. 4. – Calibration curves of thermoluminescent dosimeters (TLDs) exposed to proton beam of nominal energy of 230 MeV. The inset shows the linear fit of the thermoluminescent response as a function of the radiation dose in the dose range 0–8 Gy.

0–15 Gy for the photon beams and 0–20 Gy for the proton beam. The linear equations and statistical parameters obtained in the dose range 0–8 Gy for each TLD set were also reported in table II in order to assess the linear behaviour below 10 Gy.

The functional forms of the dose response curves in the photon field were comparable with those reported in previous works for 6 MV photon beam [7, 8]. Comparing the statistical parameter R^2 of linear and quadratic fits, the best-fitted model was the second-order polynomial as we expected in the range 0–15 Gy. A linear behaviour characterizes the dose response curves in the 0–8 Gy dose range as assessed by a value of R^2 very close to 1. A similar trend was found in the proton field (tables II and table III).

In particle beam therapy, the knowledge of the beam profile, characterized by finite ion beam range determining the position of the Bragg peak is crucial for a correct positioning of the dosimeters. This issue is even more important when referring to the correct patient position so that pre-treatment and *in vivo* dose verification methods play a key role in identifying the inaccuracies in dose delivering. Furthermore, several studies report the LET dependence of the TLD response by track structure theory and the need of correction for energy dependence response [6, 37-39]. De Zullo *et al.* [40] assessed the difference between dose measured by ionization chamber and TLD showing a minimal deviation, especially in the distal fall-off region of a Bragg peak. That is, in the proton field it is necessary to optimize the dosimeters performance and accuracy of dose measurement. To reduce the impact of the positioning inaccuracy on the absorbed dose and to ensure the reproducibility of the experiment, the set-up configuration was such that the TLD plan position falls in the flatness region of the Spread-out Bragg peak (SOBP), along the descent region of the beam profile. Few studies reported calibration of TLDs in the proton field used for measurements of dose distribution in clinical *in vivo* dosimetry [38]. The obtained results were comparable with that obtained by Sabini *et al.* that investigated the dose response function of TLD-100 exposed to a 62 MeV proton beam [38].

TABLE II. – *Best-fit equations and statistical parameters for linear and quadratic dose response models in the dose range 0–15 Gy for each TLD set for 6 MV X-rays, 15 MV X-rays and 230 MeV proton (p) beams. Abbreviations: TL = thermoluminescent signal; d = dose; SE = Standard Error; Adj = Adjusted; R = Correlation coefficient.*

	Model								
	Linear				Quadratic				
	$TL = \alpha + \beta_1 d$	SE_α (μC)	$SE_{\beta 1}$ (μC/Gy)	Adj. R^2	$TL = \alpha + \beta_1 d + \beta_2 d^2$	SE_α (μC)	$SE_{\beta 1}$ (μC/Gy)	$SE_{\beta 2}$ (μC/Gy^2)	Adj. R^2
TLD set	X-6 MV Dose range: 0–15 Gy								
A	$TL = -2 + 5.7d$	1	0.2	0.9933	$TL = 0.3 + 4.1d + 0.11d^2$	0.8	0.3	0.02	0.9988
B	$TL = -2 + 6.1d$	1	0.2	0.9953	$TL = 0.1 + 4.7d + 0.10d^2$	0.7	0.3	0.02	0.9993
C	$TL = -2 + 6.6d$	2	0.2	0.9939	$TL = 0.1 + 4.7d + 0.13d^2$	0.5	0.2	0.02	0.9996
	X-15 MV Dose range: 0–15 Gy								
A	$TL = -2 + 5.8d$	2	0.2	0.9914	$TL = 0.4 + 3.8d + 0.140d^2$	0.5	0.2	0.013	0.9996
B	$TL = -2 + 6.0d$	1	0.2	0.9953	$TL = 0.2 + 4.4d + 0.11d^2$	0.7	0.3	0.02	0.9991
C	$TL = -2 + 6.6d$	1	0.2	0.9945	$TL = 0.2 + 4.6d + 0.121d^2$	0.5	0.2	0.014	0.9996
	p-230 MeV Dose range: 0–20 Gy								
A	$TL = -3 + 5.3d$	2	0.2	0.9923	$TL = -0.1 + 3.9d + 0.07d^2$	0.8	0.2	0.01	0.9992
B	$TL = -4 + 5.7d$	2	0.2	0.9904	$TL = 0.5 + 4.0d + 0.093d^2$	0.4	0.1	0.005	0.9998
C	$TL = -2 + 5.8d$	1	0.1	0.9981	$TL = -0.7 + 5.1d + 0.037d^2$	0.6	0.2	0.008	0.9996

TABLE III. – *Best-fit equations and statistical parameters for linear dose response model in the dose range 0–8 Gy for each TLD set for 6 MV X-rays, 15 MV X-rays and 230 MeV proton (p) beams. Abbreviations: TL = thermoluminescent signal; d = dose; SE = Standard Error; Adj = Adjusted; R = Correlation coefficient.*

	Dose range: 0–8 Gy			
	Linear model			
	$TL = \alpha + \beta_1 d$	SE_α (μC)	$SE_{\beta 1}$ (μC/Gy)	Adj. R^2
TLD set	X-6 MV			
A	$TL = -0.6 + 5.18d$	0.5	0.12	0.9977
B	$TL = -0.8 + 5.6d$	0.2	0.6	0.9967
C	$TL = -0.5 + 5.67d$	0.3	0.07	0.9994
	X-15 MV			
A	$TL = -0.5 + 5.02d$	0.5	0.12	0.9976
B	$TL = -0.5 + 5.44d$	0.5	0.14	0.9974
C	$TL = -0.3 + 5.48d$	0.2	0.05	0.9974
	p-230 MeV			
A	$TL = -0.6 + 4.55d$	0.8	0.15	0.9957
B	$TL = -0.6 + 4.9d$	0.6	0.1	0.9983
C	$TL = -0.9 + 5.42d$	0.7	0.12	0.9981

The linear region allowed enabling the use of TLD sets in hypofractionated treatment schedule with single fraction up to 10 Gy. This aspect is crucial in modern radiation treatment techniques that deliver high dose level on the target with a significant dose step to reduce as much as possible irradiation of the organs at risk. Clinical protocols for standard treatment are based on International Commission on Radiation Units and Measurements (ICRU) recommendations that stated that dose delivered to a target volume in the patient must be within -5% to 7% of the prescribed dose [25, 41]. Thus, accurate *in vivo* dosimetry is essential to guarantee adequate dose to treat the tumour and a safe and accurate photon/proton beam delivery at the same time. To date, although available publications address QA procedures for proton radiotherapy [42-45] it is hard to have a comprehensive and standard protocol because of the variety of the delivery systems and tools installed in the widespread proton therapy centres.

The results of the present study, in the context of advanced radiotherapy modalities, using several energies and different radiation quality beams, showed the potential application of TLD-100 for *in vivo* dosimetry. TLD-100, after proper calibration in the specific clinical setting, are suitable for dosimetry in modern radiotherapy treatments both in standard and hypo-fractionation schedule in which high dose levels for fraction are employed.

4. – Conclusions

Thermoluminescent dosimeters are well-established devices for dose verification in radiotherapy clinical practice. However, prior to include TLDs in the quality assurance protocol they need to be calibrated with the radiation beams in use. In this study, three sets of TLDs-100 were characterized and calibrated with 6 MV and 15 MV photon beams and 230 MeV proton beam. The results showed a linear trend of thermoluminescent response as a function of the delivered dose in the dose range 0–8 Gy whereas for higher dose level a quadratic model fits better than a linear one the experimental points. This study reports a characterization of TLDs-100 enabling their use in facilities today employed for radiotherapy with photon and proton beams. We demonstrated the potential of TLDs for *in vivo* dosimetry in advanced treatment modalities where quality dose verification is essential to guarantee the correct delivery of the dose to the patient.

REFERENCES

[1] Mckinlay A. F., *Medical Physics Handbooks* (Higler A., Bristol) 1981.
[2] Kron T., *Australas. Phys. Eng. Sci. Med.*, **17** (1994) 175.
[3] Kron T., *Australas. Phys. Eng. Sci. Med.*, **18** (1995) 1.
[4] Kry S. F. *et al.*, *Med. Phys.*, **47** (2020) e19.
[5] Costa A. M. *et al.*, *Appl. Radiat. Isot.*, **68** (2010) 760.
[6] Kato T., *Radiat. Environ. Med.*, **8** (2019) 59.
[7] Liuzzi R. *et al.*, *Dose Response*, **18** (2020) 1559325819894081.
[8] Liuzzi R. *et al.*, *PLoS One*, **10** (2015) e0139287.
[9] Ernst M. *et al.*, *Dentomaxillofac. Radiol.*, **46** (2017) 20170047.
[10] Giansante L. *et al.*, *J. Appl. Clin. Med. Phys.*, **20** (2019) 308.
[11] Mettivier G. *et al.*, *Radiat. Prot. Dosim.*, **175** (2017) 473.
[12] Baumert B. G. *et al.*, *Int. J. Radiat. Oncol. Biol. Phys.*, **60** (2004) 1314.
[13] Taylor A. and Powell M. E., *Cancer Imaging*, **4** (2004) 68.
[14] Webb S., *Lancet Oncol.*, **1** (2000) 30.
[15] Durante M. and Loeffler J. S., *Nat. Rev. Clin. Oncol.*, **7** (2010) 37.
[16] Koehler A. M. and Preston W. M., *Radiology*, **104** (1972) 191.
[17] Levin W. P. *et al.*, *Br. J. Cancer*, **93** (2005) 849.
[18] Ray S. *et al.*, *Int. J. Part. Ther.*, **5** (2018) 15.
[19] Vitti E. T. and Parsons J. L., *Cancers*, **11** (2019) 946.
[20] Durante M. *et al.*, *Int. J. Radiat. Biol.*, **73** (1998) 253.
[21] Durante M. *et al.*, *Nucl. Instrum. Methods B*, **94** (1994) 251.
[22] D'avino V. *et al.*, *Radiat. Oncol.*, **10** (2015) 80.
[23] Emami B. *et al.*, *Int. J. Radiat. Oncol. Biol. Phys.*, **21** (1991) 109.
[24] Tommasino F. *et al.*, *Acta Oncol.*, **56** (2017) 730.
[25] International Commission on Radiation Units and Measurements (ICRU), *Determination of Absorbed Dose in a Patient Irradiated by Beams of X or Gamma Rays in Radiotherapy Procedures* (ICRU, Washington) 1976.
[26] Kutcher G. J. *et al.*, *Med. Phys.*, **21** (1994) 581.

[27] Kry S. F. *et al.*, *Med. Phys.*, **44** (2017) e391.
[28] Essers M. and Mijnheer B. J., *Int. J. Radiat. Oncol. Biol. Phys.*, **43** (1999) 245.
[29] Troncalli A. J. and Chapman J., *Med. Dosim.*, **27** (2002) 295.
[30] Chen R. and Mckeever S. W. S., *Radiat. Meas.*, **33** (2001) 475.
[31] Massillon-Jl G. *et al.*, *J. Phys. D.: Appl. Phys.*, **39** (2006) 262.
[32] Tommasino F. *et al.*, *Phys. Med.*, **58** (2019) 99.
[33] Rudén B. I., *Acta Radiol. Ther. Phys. Biol.*, **15** (1976) 447.
[34] Furetta C., *Handbook of Thermoluminescence* (World Scientific Pub., River Edge, NJ) 2003.
[35] Chen R. and Mckeever S. W. S., *Radiat. Meas.*, **23** (1994) 667.
[36] Li K. *et al.*, *Radiat. Res.*, **99** (1984) 465.
[37] Skopec M. *et al.*, *Radiat. Prot. Dosim.*, **101** (2002) 99.
[38] Sabini M. G. *et al.*, *Radiat. Prot. Dosim.*, **101** (2002) 453.
[39] Chu T. C. *et al.*, *Appl. Radiat. Isot.*, **55** (2001) 679.
[40] Zullo J. R. *et al.*, *Med. Dosim.*, **35** (2010) 63.
[41] International Commission on Radiation Units and Measurements (ICRU), *Prescribing, Recording, and Reporting Photon Beam Therapy* (ICRU, Bethesda, MD) 1999.
[42] Radiation Therapy Committee American Association of Physicists in Medicine, *Protocol for Heavy Charged-Particle Therapy Beam Dosimetry* (American Institute of Physics, Inc., USA) 1986.
[43] Vynckier S. *et al.*, *Radiother. Oncol.*, **20** (1991) 53.
[44] International Commission on Radiation Units and Measurements (ICRU), *Clinical Proton Dosimetry* (ICRU, Bethesda, MD) 1998.
[45] Karger C. P. *et al.*, *Phys. Med. Biol.*, **55** (2010) R193.